Available online at www.sciencedirect.com

SCIENCE DIRECT®

ELSEVIER

Physica C 412–414 (2004) 1401–1405

PHYSICA C

www.elsevier.com/locate/physc

Characteristics of two-stacked intrinsic Josephson junctions with a submicron loop on a $Bi_2Sr_2CaCu_2O_{8+\delta}$ (Bi-2212) single crystal whisker

S.-J. Kim [a,b,*], T. Hatano [b], G.-S. Kim [a], H.-Y. Kim [c], M. Nagao [b], K. Inomata [b], K.-S. Yun [b], Y. Takano [b], S. Arisawa [b], A. Ishii [b], S. Takahashi [d], J. Chen [d], K. Nakajima [d,e], T. Yamashita [b,e]

[a] *School of Mechanical Engineering, Cheju National University, Cheju 690-756, South Korea*
[b] *National Institute for Materials Science (NIMS), Tsukuba 305-0047, Japan*
[c] *Tongmyoung University of Information Technology, Pusan 608-711, South Korea*
[d] *Research Institute of Electrical Communication, Tohoku University, Sendai 980-8577, Japan*
[e] *Faculty of Science and Technology, Hirosaki University, Hirosaki 036-8561, Japan*

Received 29 October 2003; accepted 13 January 2004
Available online 11 June 2004

Abstract

We report on serial dc superconducting quantum interference devices (dc SQUIDs) arrays of two-stacked intrinsic Josephson junctions (IJJs) on a $Bi_2Sr_2CaCu_2O_{8+\delta}$ (Bi-2212) whisker with a submicron hole fabricated by a 3-D focused ion beam (FIB) etching method. The junction area, the number of elementary junctions, and the loop area of the SQUIDs are 3, 20, and 0.42 μm^2, respectively. The SQUIDs show typical *I–V* characteristics of IJJs with a critical current I_C of 12 A at 4.2 K. The modulation parameter $\beta_L (= 2I_C L/\Phi_0)$ is 6.4, and the inductance L of the SQUID is 1120 pH. That includes the inductances of the elementary junction around a SQUID loop. In a strong magnetic field, the Fraunhofer pattern is obtained and well fitted to the calculated value from the junction size; $\Delta B = \Phi_0/tW$; t is the interlayer distance; and W is the junction width. In a low magnetic field, modulation depth of approximately 10% of the I_C corresponding to the value of β_L is observed. The modulation period of 80 G approximately agrees with the value calculated from the SQUID.

PACS: 74.72.Dn; 74.80.Dm
Keywords: $Bi_2Sr_2CaCu_2O_{8+\delta}$ (Bi-2212); Intrinsic Josephson junction; Dc SQUID

1. Introduction

Rapid progress has been made in the improvement of high-T_c superconducting (HTS) Josephson junctions and superconducting quantum interference devices (SQUIDs) playing a key role in

* Corresponding author. Address: Faculty of Mechanical Energy Production, College of Engineering, Cheju National University, 1 Ara 1-dong, Jeju, Jeju-do 690-756, South Korea. Tel.: +82-64-754-3715(direct)/3710(message); fax: +82-64-756-3886.

E-mail address: kimsangj@cheju.ac.kr (S.-J. Kim).

0921-4534/$ - see front matter
doi:10.1016/j.physc.2004.01.162

superconducting electronics. Most HTS Josephson devices reported to date are based upon grain-boundary weak links like step edge, bicrystal or biepitaxial junctions [1–4]. On top of that intrinsic Josephson junctions discovered in 1992 have been studied actively for their potential application in new generation devices [5–7]. Among HTS materials, $Bi_2Sr_2CaCu_2O_{8+\delta}$ (Bi-2212) have alternate layers of superconductors and insulator in their crystal structures with high anisotropic resistivity showing Josephson current along *c*-axis. Josephson current couples with the electromagnetic field result in the Josephson plasma in the intrinsic Josephson stack in the crystal. There have been a few of experimental reports that showing the existence of the Josephson plasma in HTS materials [8,9]. The serial dc SQUID arrays of two-stacked intrinsic Josephson junctions (IJJs) on a $Bi_2Sr_2CaCu_2O_{8+\delta}$ (Bi-2212) is one of powerful methods for obtaining the high output voltage of the SQUIDs and finding the excitation of Josephson plasma by inductive coupling of layer intrinsic Josephson junction structures [10]. However, the characteristics of serial dc SQUID arrays of two-stacked IJJs have not been observed until now because of the lack of a fabrication method.

Here we introduce a 3-D fabrication method of the SQUIDs on a Bi-2212 single crystal whisker without any complicated processes and investigate the dc Josephson effect on the SQUID by weak and strong external magnetic field.

2. Experimental

In this experiment, we used a Bi-2212 single-crystal whisker grown by a Pb-free method; these crystal whiskers have been characterized as a very high-quality crystalline object [11]. The Bi-2212 stack showed zero-resistance transition temperatures in the range of 75–85 K and a critical current density J_C of about 10^3 A/cm^2 at 4.2 K. Four contacts were prepared with silver paste for electrical measurements. To decrease the contact resistance, the contact was annealed in an oxygen flow at 450 °C. The magnetic field dependence and electrical transport properties were measured using PPMS from Quantum Design Co.

For etching, we used a commercial FIB machine, the SMI-9800 (SE). This apparatus uses a focused Ga^+ ion beam with a maximum energy of 30 keV. We installed the specifically designed 3-D lateral etching system by using an automatic sample stage tilting up to 90° [12]. Thus, we patterned the bridge width from the top direction and the junction layer length from the lateral direction by tilting the sample stage up to 90°. The exact stack size was etched by scanning the sample images from the top and lateral view. As far as we know, this was, until now, the only possible method for making a dc-SQUID structure using an intrinsic Josephson junction stack.

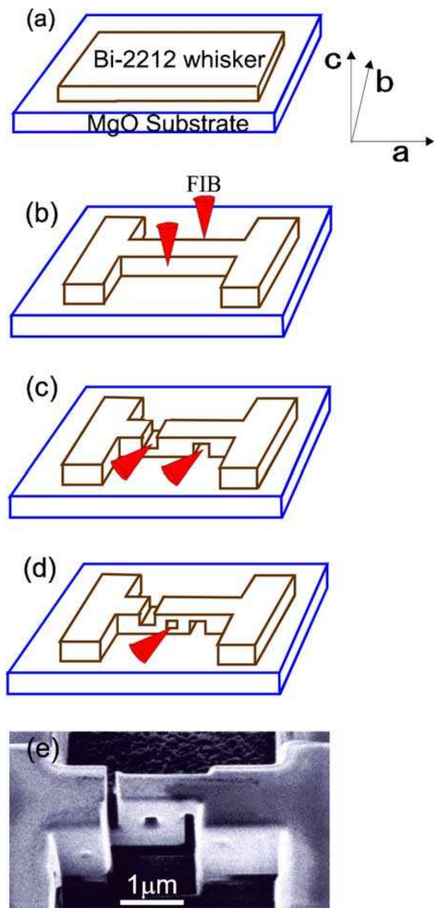

Fig. 1. Fabrication process of Bi-2212 dc SQUID fabricated by a 3-D focused ion beam (FIB) etching method (a)–(d) and the tilt view of one of the fabricated samples.

The steps of the fabrication process using FIB etching are shown in Fig. 1(a)–(d). As the first step, the whiskers were fixed to the sample holder of the FIB etching machine. A bridge with a width of 1–2 μm was etched in a micro area depending on the required junction size, and a full depth of whisker thickness was etched in the required stack area (Fig. 1(b)). After this, the substrate was turned over up to 90° by tilting the sample stage automatically. Then, two grooves of a similar depth were etched in the whole length, and the distance between the grooves was offset according to the required junction size (Fig. 1(c)). Finally, a hole of rectangular geometry of a hole was etched in the whole length (Fig. 1(d)). Fig. 1(e) shows the tilt view of one of the fabricated samples.

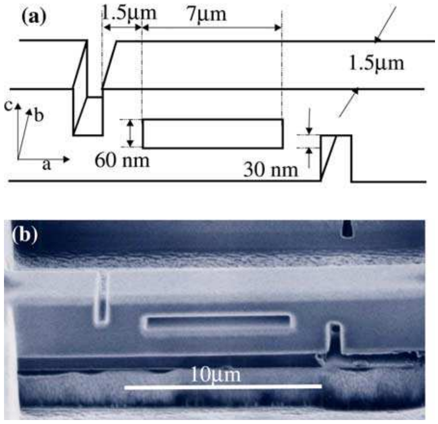

Fig. 2. Scheme (a) and SIM photograph (b) of an intrinsic Josephson junction dc SQUID using a Bi-2212 single-crystal whisker. The bridges are 2 μm wide; the size of the SQUID hole is 0.42 μm^2.

3. Results and discussion

Recently we observed the Fraunhofer pattern with a period of 1 T using a 1.4×1.4 μm^2 single junction stack [13]. The highly suppressed multi-branch structure in the I–V curves of a single junction shows the field dependence of a I–V curve although the behavior is not completely explained. The Fraunhofer pattern is obtained and well fitted to the calculated value from the junction size; $\Delta B(=\Phi_0/tW)$; t is the interlayer distance; and W is the junction width.

In our preliminarily research, we fabricated a dc SQUID from a junction area of 1×1 μm^2, a junction height of 0.35 μm, and a loop area of 0.7 μm^2 and tried to observe an interference pattern in the low and high magnetic fields. The critical current I_C of the stack was 6.4 μA. However, we could not find the magnetic field modulation period of the critical current in the weak magnetic field. We assume that the contribution of the multi-elementary Josephson junction in a loop working as an equivalent inductance induces a high value of $\beta_L(=2I_CL/\Phi_0)$ [14]. The junction inductance per single junction is as follows: $L_J=\Phi_0/2\pi I_C=103$ pH. From the elementary number of junction 460, $\beta_L=732$. In this case, an interference pattern will be suppressed and will be smaller than 1% [15]. Therefore, the modulation period is difficult to observe.

Here, we designed the dimensions of dc SQUID using mainly the modulation parameter β_L. The dimensions of dc SQUID and the photo are shown in Fig. 2(a) and (b), respectively. Some white parts around a loop in Fig. 2(b) may be from over-etching.

We designed the height of both junction stacks to be 0.03 μm to achieve an elementary junction number of 20 junctions; the junction area was set to be 3 μm^2. The loop area was 0.42 μm^2 to achieve a modulation period of 50 G. The calculated inductance from the loop area, $L_M=1.25\mu_oD$ [16], is 20 pH, where D is the SQUID loop diameter and μ_o the vacuum permeability. The modulation parameter β_L is 1.2, and 40% modulation depth is expected when we disregard junction inductance. Fig. 3(a) shows the I–V characteristics of a fabricated dc-SQUID at the low-bias region. The SQUID shows the typical I–V characteristics of IJJs with an I_C of 12 A at 4.2 K. The I_CR_N product of the SQUID is 14.4 mV, and R_N ($\approx$1.2 kΩ) is the normal resistance of the device. Also, when we considered the junction inductance ($\approx$1100 pH), β_L is 6.4, and approximately 8% of the modulation depth is expected. Magnetic field dependence on I–V curves around zero bias region shows in Fig. 3(b) and (c). Fig. 3(b) shows the modulation of I_C when we apply the magnetic field was biased in the

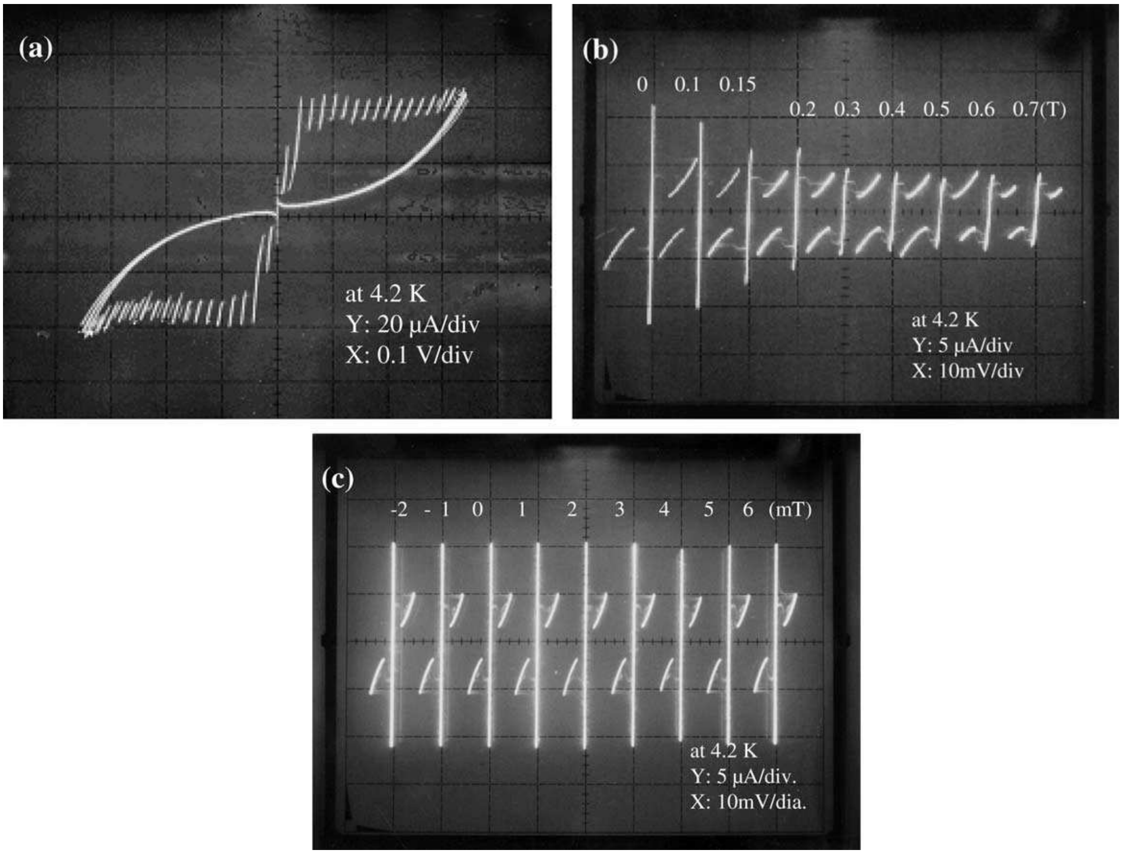

Fig. 3. I–V characteristics of the 0.42 μm^2 loop SQUID around the low-bias region at 4.2 K (a). Magnetic field dependence of the critical current of the dc SQUID in larger magnetic fields (b) and in smaller magnetic fields (c).

range of 0–1.7 T. The modulation characteristics of a weak magnetic field in the range of mT are shown in Fig. 3(c).

In strong fields, the Fraunhofer pattern of modulation periods 0.345 T was observed. Those experimental plots correspond to the theoretical values as shown in Fig. 4(a). Fig. 4(b) shows the plots of I_C modulation as a function of the applied magnetic field in a low magnetic field. Approximately 10% of the I_C modulation corresponding to the value of β_L is observed. The modulation period of 80 G approximately agrees with the calculated value from the SQUID.

Until now, we explained that these phenomena might be from the equivalent junction inductance of a multi intrinsic Josephson junction. The other possibility might also be explained by the quantum effect in the superconducting closed loop containing a series of Josephson junctions [17].

In the case of SIS IJJ, the output voltage will be much higher than a single junction because the output voltage will mainly depend on the $I_C R_N$ product. In other words, the series arrays of the junction increase the $I_C R_N$ product because the I_C is constant, while the R_N increases. Improving the SQUID performance, we expect that the FIB-fabricated IJJs could be used as a part of an integrated device.

This device fabrication method is possibly applicable to circuits such as the small-loop SQUIDs for use in digital circuits.

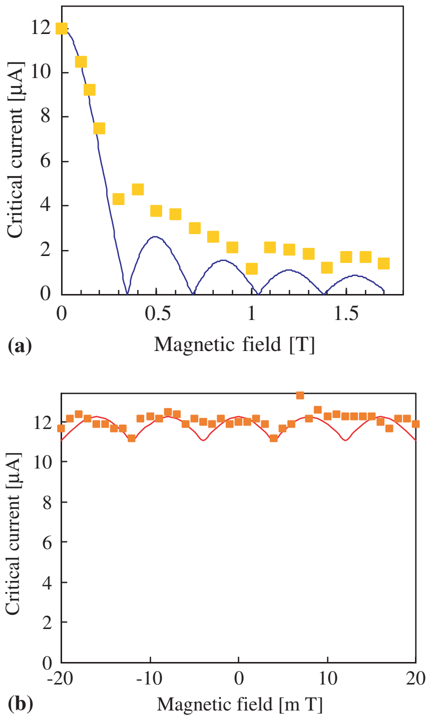

Fig. 4. Experimental plots of I_C modulation correspond to the theoretical values. Modulation of I_C when we apply a larger magnetic field (a) and in small magnetic fields (b).

4. Summary

We investigated the characteristics of micromachined dc SQUID formed by IJJs. The dc SQUID junctions produced by FIB etching were uniform and reproducible, with most of the junctions displaying magnetic field dependence in a strong magnetic field.

The FIB-etched dc SQUID junctions showed a magnetic field dependence of I–V curves. In the case of the 460-IJJs, we observed the Fraunhofer pattern, which appears as a single IJJ, although we did not observe an interference pattern. This may be caused by the multi-junction inductance around a loop related to the modulation parameter β_L. A small number of elementary junctions need to be made in a loop in order to find the interference pattern of IJJ dc SQUID. The observed modulation period and depth of magnetic field correspond to the designed values when we consider the equivalent inductances around a loop.

Acknowledgements

This work was supported by a grant from the academic research fund of the Cheju National University Development Foundation.

References

[1] K. Char, M.S. Colclough, L.P. Lee, K. Zaharchuk, Appl. Phys. Lett. 59 (1991) 2177.
[2] D. Dimos, P. Chaudhari, J. Mannhart, Phys. Rev. B 41 (1990) 4038.
[3] J. Gao, Yu. Boguslavskij, B.B.G. Klopman, D. Terpstra, G.J. Gerritsma, H. Rogalla, Appl. Phys. Lett. 59 (1991) 2754.
[4] R.H. Ono, J.A. Beall, M.W. Cromar, T.E. Harvey, M.E. Johansson, C.D. Reintsema, D.A. Rudman, Appl. Phys. Lett. 59 (1991) 1126.
[5] R. Kleiner, F. Steinmeyer, G. Kunkel, P. Muller, Phys. Rev. Lett. 68 (1992) 2394.
[6] H.L. Johnson, G. Hechtfischer, G. Gotz, R. Kleiner, P. Muller, J. Appl. Phys. 82 (1997) 756.
[7] S.-J. Kim, Yu.I. Latyshev, T. Yamashita, Appl. Phys. Lett. 74 (1999) 1156.
[8] K. Tamasaku, S. Uchida, S. Tajima, Phys. Rev. B 53 (1996) 14558.
[9] Y. Matsuda, M.B. Gaifullin, K. Kumagai, K. Kadowaki, T. Mochiku, Phys. Rev. Lett. 75 (1995) 4512.
[10] V.K. Kaplunenko, J. Mygind, N.F. Pedersen, A.V. Ustinov, J. Appl. Phys. 73 (1993) 2019.
[11] T. Hatano, Y. Takano, S. Arisawa, A. Ishii, K. Togano, A. Fukuyo, IEEE Trans. Appl. Supercond. 11 (2001) 2846.
[12] S.-J. Kim, T. Yamashita, J. Appl. Phys. 89 (2001) 7675.
[13] Yu.I. Latshev, V.N. Pavlenko, S.-J. Kim, T. Yamashita, L.N. Bulaevskii, M.J. Graf, A.V. Balatsky, N. Morozov, M.P. Maley, Physica C 341–348 (2000) 1499.
[14] C.D. Tesche, J. Clarke, J. Low Temp. Phys. 29 (1997) 301.
[15] A. Barone, G.释ernò, Physics and Applications of the Josephson Effect, Wiley, New York, 1982.
[16] T. Van Duzer, C.W. Turner, Principles of Superconducting Devices and Circuits, Elesiver, New York, 1981.
[17] T. Yamashita, Y. Ogawa, Y. Onodera, J. Appl. Phys. 50 (1979) 3547.